

# Comparison of some existing parametric models for magnetorheological fluid dampers

İ Şahin<sup>1</sup>, T Engin<sup>2</sup> and Ş Çeşmeci<sup>2</sup>

<sup>1</sup> Akyazı Vocational School, University of Sakarya, Akyazı, Sakarya, Turkey

<sup>2</sup> Department of Mechanical Engineering, University of Sakarya, Sakarya, Turkey

E-mail: [isahin@sakarya.edu.tr](mailto:isahin@sakarya.edu.tr) and [ismailsahin@yahoo.com](mailto:ismailsahin@yahoo.com)

Received 8 October 2009, in final form 6 January 2010

Published 3 February 2010

Online at [stacks.iop.org/SMS/19/035012](http://stacks.iop.org/SMS/19/035012)

## Abstract

Magnetorheological dampers have received a great deal of attention in the last two decades due to their being a potential technology to conduct semi-active control. It is therefore vitally important to understand the dynamic behavior of such devices whose nonlinear hysteresis is a rather complicated phenomenon. Hence, this paper aims at conducting a comparative evaluation of the currently available parametric models that have been widely used to develop control algorithms that take maximum advantage of the unique features of MR dampers. The comparisons showed that the simple algebraic parametric models exhibited considerably better predictions than the much more complicated ordinary differential parametric models.

(Some figures in this article are in colour only in the electronic version)

## 1. Introduction

Magnetorheological (MR) fluids are suspensions of magnetically polarizable micron-sized tiny particles dispersed in a carrier liquid such as mineral or silicon oil. When an external magnetic field is applied to the fluid, the suspended particles in the fluid form chains and the suspension becomes like a semi-solid material due to the increase in the apparent viscosity. Under the magnetic field, an MR fluid behaves like a non-Newtonian fluid with controllable viscosity. However, if the magnetic field is removed, the suspension turns into a Newtonian fluid in a few milliseconds, and the transition between these two phases is highly reversible, which provides the unique feature of magnetic field controllability of the flow of MR fluids.

Typically, an MR damper consists of a hydraulic cylinder, magnetic coils and MR fluid offering design simplicity. In addition to field controllability and design simplicity, MR dampers have many other advantages such as they (i) require relatively very low power input, (ii) produce high yield stress up to 100 kPa, (iii) can be stably operated in a wide range of temperature (−40–150 °C) and (iv) MR fluids are not toxic and are insensitive to impurities [1]. Moreover, without the magnetic field the MR damper can work in a fail-safe

mode, i.e. as a classical passive dashpot. Owing to these advantages, MR dampers have received much interest from different fields of applications including, but not limited to, automotive suspensions, seismic vibration mitigation, large bridges vibration control, knee prosthesis and so on [2].

Effective control of an MR damper mainly depends on understanding its nonlinear hysteretic behavior under an applied magnetic field. Therefore, one needs to develop control algorithms that take maximum advantage of the unique features of MR dampers, and the models must adequately characterize the intrinsic nonlinear behavior of these devices [3]. The existing models can be classified into two main categories as parametric and non-parametric. Non-parametric models are able to model the MR damper behavior in such a way that the model parameters do not necessarily have physical meanings [4]. Some of the non-parametric models are Chebyshev polynomials [5, 6], neural networks [7–10] and neuro-fuzzy [11, 12]. A literature survey would indicate that, although non-parametric models can effectively represent MR damper behavior, they are highly complicated and demanding massive experimental datasets for model validation.

Parametric models, on the other hand, are the most desirable ones as their parameters have some physical

meaning [4]. These models consist of some mechanical elements such as linear viscous, friction, springs, etc. Parameters associated with these mechanical elements are estimated by comparing the models with experimental results. One of the earliest parametric models is the Bingham visco-plastic model developed by Stanway *et al* [13]. In this model, a Coulomb friction element is placed in parallel with a linear viscous one. Spencer *et al* [3] demonstrated that, although this model could reasonably describe the force–displacement behavior, it could not capture the observed nonlinear force–velocity characteristic adequately. A visco-elastic-plastic model based on the Bingham visco-plastic model was proposed by Gamota and Filisko [14]. It was constructed by adding a standard linear solid model in series with the original Bingham model. Wereley *et al* [15] proposed a nonlinear hysteretic biviscous model, which is an extension of the nonlinear biviscous model having an improved representation of the pre-yield hysteresis first suggested by Kamath and Wereley [16]. Wilson *et al* [12] reported that this model, like the previously discussed models, could describe the force–displacement behavior successfully; however, it could not readily replicate the force roll-off in low force–velocity hysteresis loops.

The nonlinear hysteretic biviscous model was extended by Li *et al* [17], who reported that the deformation was visco-elastic in the pre-yield region and visco-plastic in the post-yield region. They also observed that the MR damper operated in the post-yield region rather than in the pre-yield region. Choi and Lee [18] proposed a polynomial model and compared the results with that of Bingham and Bouc–Wen models, and proved that their model predicted the hysteresis behavior more closely under various conditions. Du *et al* [10] reported that the polynomial model was a convenient and effective choice which could realize the inverse dynamic of the MR damper in an analytical form, and was easy to achieve the desirable damper force in an open-loop control system. However, the polynomial model cannot characterize the behavior of the MR damper favorably in the relatively low velocity region since this model does not include variables characterizing the pre-yield property of the damper force. Gavin *et al* [19] developed a hyperbolic tangent function to predict MR damper force. They indicated that, as the model did not have a dynamic character, it could not capture the frequency-dependent visco-elastic behavior, but the model results corresponded to the experimental results.

The most extensively used model for modeling hysteretic systems is the Bouc–Wen model. The Bouc–Wen model was initially proposed by Bouc early in 1971 and generalized by Wen [20] in 1976 and since then it has been called the Bouc–Wen model. The general Bouc–Wen model predicts the force–displacement behavior of the damper well, and it possesses force–velocity behavior that more closely resembles the experimental data. However, similar to the Bingham model, the nonlinear force–velocity response of the Bouc–Wen model does not roll-off in the region where the acceleration and velocity have opposite signs and the magnitude of the velocities are relatively small. Due to this reason, Spencer *et al* [3] proposed a modified Bouc–Wen model (also called the phenomenological model) to better predict the damper

response in this region. They estimated the parameters of the modified Bouc–Wen model and compared the results between predicted response and corresponding experimental data. The proposed model predicted the behavior of the damper very well in all regions including the region with low velocities and the acceleration and velocity have opposite signs.

The characteristic parameters in the Bouc–Wen model were not functions of the frequency, amplitude and current excitations; therefore, the estimated parameters could characterize the behavior of the tested MR damper under specific excitation conditions and must be re-evaluated if a different combination of excitation parameters is desired, which actually could be extremely cumbersome and computationally expensive. In this context, to better characterize the hysteresis phenomenon of the MR damper, Spencer *et al* [3] generalized their proposed modified model for fluctuating magnetic fields. By this, they were able to describe the behavior of the MR damper at any current excitation, and thus magnetic field. This is, of course, crucially important for developing an effective control algorithm for the damper. For the same purpose, Dominguez *et al* [21] proposed a new hysteresis model based on the original Bouc–Wen model to incorporate not only the current excitation as done by Spencer *et al* [3], but also frequency and amplitude. By this, they enabled the designer to predict the hysteresis force more efficiently and accurately under different excitation conditions. Zhou *et al* [22] proposed a more simple and effective modified model, which was first suggested by Dahl [23]. In this model, the Dahl hysteresis model instead of the Bouc–Wen model is adopted to simulate Coulomb force to avoid the determination of too many parameters. A relatively novel simple algebraic model was suggested by Kwok *et al* [24]. This model, which is similar to the one proposed by Gavin *et al* [19], utilized a hyperbolic tangent function to represent the hysteretic characteristic of MR dampers. They noted that their model was computationally efficient in the context of parameter identification and subsequent inclusion in controller design and implementation. Another notable algebraic model was used by Guo and Hu [25], and they demonstrated that the algebraic model could successfully capture the nonlinear characteristics of the MR damper.

Gavin [26] designed, manufactured and tested ER dampers, and he used both evolutionary and algebraic models to represent the dynamic behavior of these dampers. He reported that the evolutionary model captured the frequency dependence well, whereas the frequency-independent algebraic model was not able to capture some details of the pre-yield behavior for the high-force device.

From the discussion above, it is clearly seen that, although various models, both parametric and non-parametric, have been proposed in the literature to represent the dynamic behavior of MR dampers, there is still no systematic comparative evaluation of these existing models with their inherent aspects. This paper aims at conducting a comparative evaluation of the most commonly used parametric models for predicting the dynamic behavior of the MR dampers. To this end, an MR damper has been designed, fabricated and tested at the Applied Fluid Mechanics Laboratory (AFML) in the

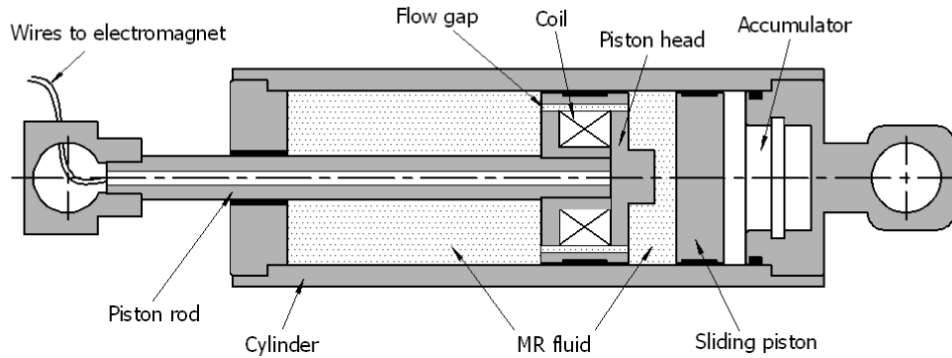


**Figure 1.** Schematic for the prototyped MR damper (SAUMRD002).

**Table 1.** Technical specifications of SAUMRD002.

Test damper specifications	
Maximum stroke	80.0 mm
Total length	270.0 mm
Cylinder diameter	40.0 mm
Shaft diameter	10.0 mm
Resistance	7 $\Omega$
Maximum input current	2.0 A

University of Sakarya. The experimental data were then used to compare the models.

So far, a comprehensive literature review has been presented. Now we continue with the experimentation on the prototyped MR damper in section 2. Then, the considered models here are reviewed briefly. After that, a comparative evaluation of all the models is given through a quantitative error analysis in the time, displacement and velocity domains. Finally, the results are discussed to present the advantages and disadvantages of each model based on their accuracy, complexity, and computational costs and time.

## 2. Test damper and experimental measurements

The MR damper (SAUMRD002) used in this work was designed and manufactured at the Applied Fluid Mechanics Laboratory (AFML), the University of Sakarya. Figure 1 shows a schematic for the prototyped SAUMRD002 MR fluid damper.

The chambers that are separated by the piston head are filled with MR fluid (MRD 122ED, Lord Corp., USA), whereas the accumulator that is used for compensating the volume changes induced by the movement of the piston rod up and down is filled with pressurized nitrogen gas. During the motion of the MR damper's piston rod, fluid flows through the annular gap opened on the piston head. Inside the piston head, a coil is wound around the bobbin shaft with a heat-resistant and electrically insulated wire. When electrical current is applied to the coil, a magnetic field develops around the piston head. The technical specifications of the test damper are given in table 1.

Experimental data of the MR damper have been acquired under the sinusoidal excitations on a mechanical scotch-yoke type Roehrig 10VS damper dynamometer. The main

components of the test set-up along with the test damper are shown in figure 2. The shock machine has its own software to collect data from the data card and use them to plot force versus time, force versus displacement and force versus velocity graphs for each test.

A programmable GWinstek PPE 3223 power supply is used to feed current to the MR damper. The machine also has an IR temperature sensor to read the temperature data during the tests. The damper is fixed to the machine via grippers as shown in figure 2. The machine excites the damper's piston rod sinusoidally, while a load cell of 22 kN measures the force on the damper and a linear variable displacement transducer (LVDT) measures the displacement of the piston rod as well as the relative velocity between the two ends of the damper. A series of tests is conducted to determine the dynamic response of the damper at current inputs of 0, 0.2, 0.4, 0.6, 0.8, 1.0, 1.5 and 2.0 A under four constant excitation velocities of 0.05, 0.1, 0.15 and 0.2 m s<sup>-1</sup>, respectively. A total of 224 tests were conducted to obtain approximately 5200 data points, which were saved by means of the shock machine's software. The data were then transferred directly to a Matlab environment in order to use them for comparative evaluation of the parametric models considered.

## 3. Some existing parametric models for MR dampers

A comparative evaluation of the presently available parametric models widely used to develop control algorithms that take maximum advantage of the unique features of MR dampers has been performed. Below, we will give brief information about these models and compare them against the test data under various input currents and maximum velocities. The parametric models under consideration in this paper can be grouped into two categories. The first category involves the solution of an evolutionary model that has a nonlinear ordinary differential equation. The second category involves the evaluation of an algebraic expression.

### 3.1. The evolutionary models

**3.1.1. General Bouc–Wen model (BW).** One of the earliest models that has been extensively used in modeling dynamic behavior of hysteretic systems is the standard Bouc–Wen

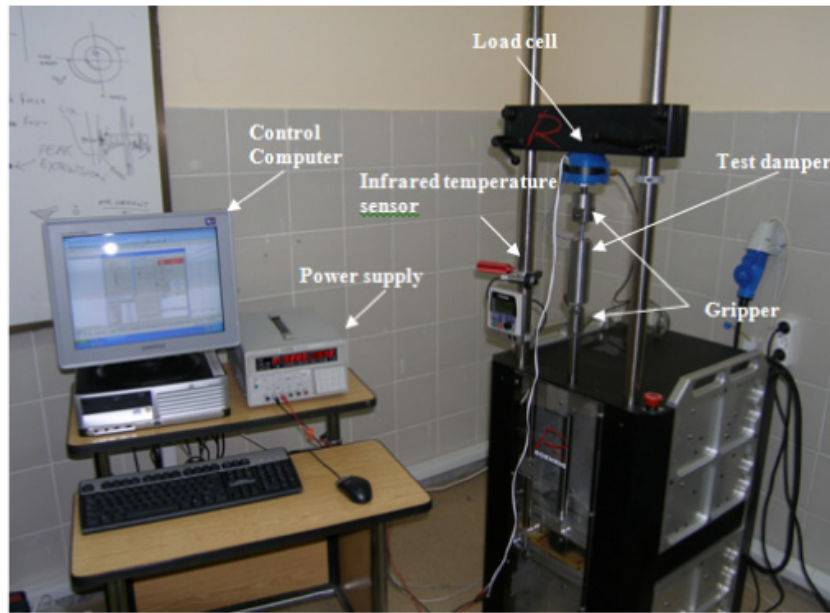


Figure 2. Photograph of the test machine with the damper under test.

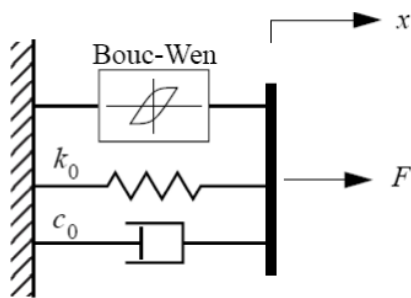


Figure 3. The Bouc–Wen model for the MR damper.

model, which is extremely versatile and can exhibit a wide variety of hysteretic behavior. The Bouc–Wen model is described by Spencer *et al* [3] as

$$F = c_0\dot{x} + k_0(x - x_0) + \alpha z \quad (1)$$

where the evolutionary variable  $z$  is governed by

$$\dot{z} = -\gamma z|\dot{x}||z|^{n-1} - \beta\dot{x}|z|^n + A\dot{x} \quad (2)$$

As stated by Spencer *et al* [3], by adjusting the parameters of the model  $\gamma$ ,  $\beta$  and  $A$ , one can control the linearity in the unloading and the smoothness of the transition from the pre-yield to the post-yield region. In addition, the force  $f_0$  due to the accumulator can be directly incorporated into the model as an initial deflection of the linear spring  $k_0$ . An illustration of this model is given in figure 3.

**3.1.2. Modified Bouc–Wen model (mBW).** Since the nonlinear force–velocity response of the Bouc–Wen model does not roll-off in the region where the acceleration and velocity have opposite signs and the magnitudes of the velocities are small, Spencer *et al* [3] proposed a modified

version of the Bouc–Wen model in order to predict the dynamic behavior of the MR damper in this region. The modified Bouc–Wen model was expressed as follows:

$$F = \alpha z + c_0(\dot{x} - \dot{y}) + k_0(x - y) + k_1(x - x_0) \quad (3)$$

where the evolutionary variable  $z$  is governed by

$$\dot{z} = -\gamma|\dot{x} - \dot{y}|z|z|^{n-1} - \beta(\dot{x} - \dot{y})|z|^n + A(\dot{x} - \dot{y}) \quad (4)$$

where

$$\dot{y} = \frac{1}{(c_0 + c_1)}\{\alpha z + c_0\dot{x} + k_0(x - y)\}. \quad (5)$$

In this modified model, the accumulator stiffness is represented by  $k_1$  and the viscous damping observed at larger velocities is represented by  $c_0$ . A dashpot, represented by  $c_1$ , is included in the model to produce the roll-off that was observed in the experimental data at low velocities,  $k_0$  is present to control the stiffness at large velocities and  $x_0$  is the initial displacement of spring  $k_1$  associated with the nominal damper force due to the accumulator. A schematic for the model is given in figure 4.

**3.1.3. Voltage-dependent modified Bouc–Wen model (vmBW).**

Spencer *et al* [3] proposed a generalized version of the model illustrated in figure 4 for fluctuating current excitations and, thus, magnetic fields. From their experimental observations, they concluded that  $\alpha$ ,  $c_1$  and  $c_0$  vary linearly with the applied input voltage and proposed the following relations:

$$\begin{aligned} \alpha(u) &= \alpha_a + \alpha_b u \\ c_1(u) &= c_{1a} + c_{1b} u \\ c_0(u) &= c_{0a} + c_{0b} u \end{aligned} \quad (6)$$

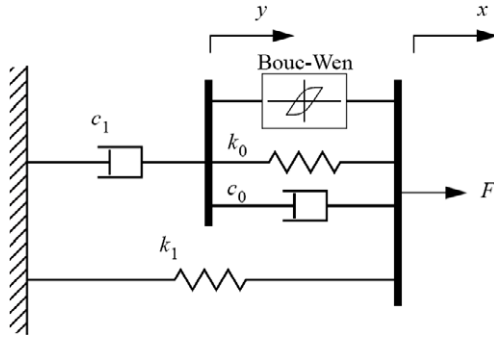


**Figure 4.** The modified Bouc–Wen model for the MR damper.

where the dynamics involved in the MR fluid reaching rheological equilibrium are accounted for through the first-order filter:

$$\dot{u} = -\eta(u - v) \quad (7)$$

and  $v$  is the applied voltage to the current driver. The optimal values of a total of 14 parameters ( $c_{0a}$ ,  $c_{0b}$ ,  $k_0$ ,  $c_{1a}$ ,  $c_{1b}$ ,  $k_1$ ,  $x_0$ ,  $\alpha_a$ ,  $\alpha_b$ ,  $\gamma$ ,  $n$ ,  $\beta$ ,  $\eta$  and  $A$ ) have to be estimated by matching experimental data and model predictions for the MR damper.

**3.1.4. Modified Dahl model (mDahl).** Zhou and Qu [22] suggested a simple and more effective modified version of the Dahl [23] model as illustrated in figure 5. In this model, the Dahl hysteresis model instead of the Bouc–Wen model was adopted to simulate Coulomb force to avoid estimating too many parameters. Moreover, the modified Dahl model was reported to be successful in capturing the force–velocity relationship in the low velocity region. In this model, the force generated by the MR damper is given by

$$F = K_0x + C_0\dot{x} + F_dz - f_0 \quad (8)$$

where  $K_0$  is the stiffness of the linear spring,  $C_0$  the damping coefficient,  $F_d$  the Coulomb force modulated by applied magnetic field,  $x$  the displacement of the MR damper and  $f_0$  the damper force caused by seals and measurement bias. In equation (8), the parameter is the nondimensional hysteretic variable governed by

$$\dot{z} = \sigma\dot{x}(1 - z \operatorname{sgn}(\dot{x})) \quad (9)$$

where  $\sigma$  determines the hysteretic loop shape. In order to calibrate the modified Dahl model under a certain applied fluctuating magnetic field, it is necessary to obtain the relationship between model parameters and applied magnetic field. This relationship is given by

$$C_0 = C_{0s} + C_{0d}u, \quad F_d = F_{ds} + F_{du} \quad (10)$$

where  $C_{0s}$  and  $F_{ds}$  are the damping coefficient and Coulomb force of the MR damper at 0 V, respectively.  $u$  is the intrinsic variable to determine the function dependence of the parameters on the applied voltage  $V$ . The relation between  $u$  and  $V$  is modeled by Spencer *et al* [3] with a first-order filter:

$$\dot{u} = -\eta(u - V) \quad (11)$$

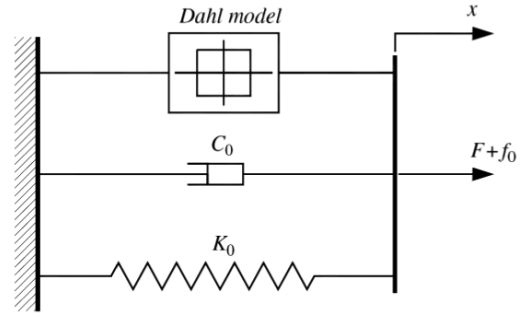


**Figure 5.** Modified Dahl model of the MR damper.

where  $\eta$  reflects response time of the MR damper, namely, a larger  $\eta$  means shorter response time.  $V$  is the applied voltage. The model involves a total of eight parameters ( $C_{0s}$ ,  $C_{0d}$ ,  $F_{ds}$ ,  $F_{du}$ ,  $K_0$ ,  $\sigma$ ,  $f_0$  and  $\eta$ ) to be determined based on the experimental data.

**3.1.5. Modified LuGre friction model (mLF).** The use of the LuGre model for representing the dynamics of an MR damper was first introduced at the 15th IFAC World Congress [27], where Jimenez *et al* [28] expressed the modified LuGre friction model (mLF) to describe MR damper dynamic behavior. This model, which is an extension of the friction model proposed by Dahl [23], has been used in a wide range of applications related to friction. Its mathematical simplicity and high accuracy makes the mLF model a good candidate in modeling and control design problems. The model is expressed as follows:

$$F = f_0 + \beta z + \gamma \dot{x} + \delta x + \varepsilon \dot{z} \quad (12)$$

$$\dot{z} = \dot{x} - \alpha |\dot{x}| z \quad (13)$$

where  $\alpha$  ( $\text{mm}^{-1}$ ),  $\beta$  ( $\text{N mm}^{-1}$ ),  $\gamma$  ( $\text{Ns mm}^{-1}$ ) and  $\varepsilon$  ( $\text{N} \cdot \text{s mm}^{-1}$ ) are generalized stiffness and damping parameters that can vary with the applied current. In addition,  $F$  (N) is the total force applied by the MR damper,  $x$  (mm) is the damper's displacement and  $z$  (mm) is related to the deformation of the MR fluid, which is actually enclosed within the damper cylinder.

## 3.2. The algebraic models

**3.2.1. Kwok model (Kwok).** Kwok *et al* [24] proposed a model that makes use of a hyperbolic tangent function to represent the hysteresis and linear functions to represent the viscous and stiffness (figure 6(a)). The model is given by

$$F = c\dot{x} + kx + \alpha z + f_0 \quad (14)$$

$$z = \tanh[\beta\dot{x} + \delta \operatorname{sgn}(x)] \quad (15)$$

where  $c$  and  $k$  are the viscous and stiffness coefficients,  $\alpha$  the scale factor of the hysteresis,  $z$  the hysteretic variable given by the hyperbolic tangent function and  $f_0$  is the damper offset. Kwok *et al* [24] pointed out that their model contains only a simple hyperbolic tangent function and is computationally efficient in the context of parameter identification and subsequent inclusion in controller design and implementation. The effect of each individual parameter on the hysteretic cycle is also illustrated in figure 6(b).

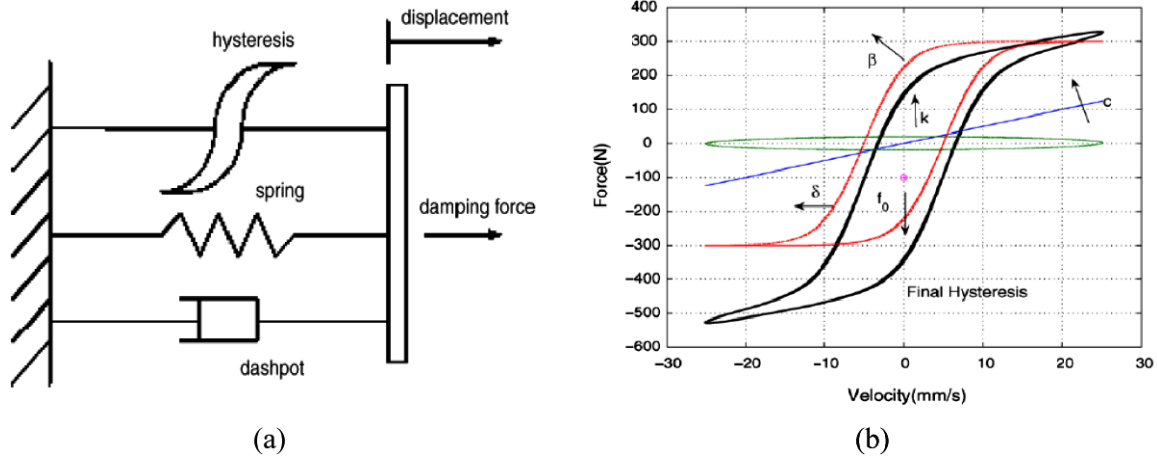


Figure 6. (a) The Kwok model. (b) The effects of each parameter involved.

3.2.2. Algebraic model (Alg). Another simple algebraic model was proposed by Guo and Hu [25] to model the hysteresis of the MR damper. The model is given by

$$F = f_0 + c_b \dot{x} + \frac{2}{\pi} f_y \arctan\{k[\dot{x} - \dot{x}_0 \operatorname{sgn}(\ddot{x})]\} \quad (16)$$

where  $f$  represents the damping force of the MR damper,  $f_0$  the pre-load of the gas accumulator,  $c_b$  the coefficient of viscous damping,  $f_y$  the yielding force,  $k$  the shape coefficient,  $\dot{x}_0$  the hysteretic velocity, and  $\dot{x}$  and  $\ddot{x}$  the input velocity and acceleration of the piston in the damper, respectively.

3.2.3. Modified algebraic model (mAlg). It has been observed that the algebraic model proposed by Guo and Hu [25] exhibited good agreement between the estimated and measured values except at lower current inputs, i.e. 0 and 0.2 A. We have reasoned that this could be presumably due to the fluid inertial force, which becomes significant at low input currents. Starting from this point, we modified the Guo model given by equation (16) by adding an inertial force term in order to improve the agreement between the simulated and experimental data. Hence, the modified algebraic model takes the following form:

$$F = f_0 + c_b \dot{x} + \frac{2}{\pi} f_y \arctan\{k[\dot{x} - \dot{x}_0 \operatorname{sgn}(\ddot{x})]\} + m\ddot{x} \quad (17)$$

where  $m$  represents a virtual mass which has to be determined based on the experimental data.

#### 4. Comparison of the parametric models against test data

In order to assess a comparative evaluation, eight parametric hysteretic models proposed in the literature have been studied. These models are widely used in order to describe the dynamic behavior of the MR dampers, and they have been generally tested for some particular sets of experimental data, and no comparative study about their accuracy is currently available. The major aim of this paper is to comparatively evaluate such existing parametric models against a relatively large test

Table 2. Normalized error norms of the parametric models under consideration in this study.

$v$ (m s <sup>-1</sup> )	0.05	0.10	0.15	0.20	Average
	$E_t$				
mDahl [22]	0.041	0.042	0.043	0.038	0.0410
Kwok [24]	0.026	0.021	0.018	0.023	0.0221
BW [3]	0.035	0.036	0.092	0.038	0.0503
mBW [3]	0.034	0.022	0.021	0.024	0.0251
vmBW [3]	0.032	0.022	0.022	0.020	0.0241
mLF [28]	0.038	0.031	0.031	0.034	0.0333
Alg [25]	0.034	0.023	0.021	0.025	0.0257
mAlg (this study)	0.035	0.022	0.021	0.016	0.0230
	$E_x$				
mDahl [22]	0.004	0.006	0.008	0.009	0.0066
Kwok [24]	0.003	0.003	0.004	0.006	0.0042
BW [3]	0.004	0.005	0.016	0.008	0.0082
mBW [3]	0.004	0.004	0.005	0.007	0.0046
vmBW [3]	0.004	0.004	0.005	0.006	0.0043
mLF [28]	0.004	0.005	0.006	0.008	0.0059
Alg [25]	0.004	0.004	0.005	0.007	0.0048
mAlg (this study)	0.004	0.003	0.004	0.004	0.0038
	$E_{\dot{x}}$				
mDahl [22]	0.018	0.036	0.056	0.064	0.0435
Kwok [24]	0.011	0.018	0.023	0.038	0.0230
BW [3]	0.015	0.031	0.122	0.065	0.0583
mBW [3]	0.015	0.019	0.025	0.038	0.0243
vmBW [3]	0.014	0.018	0.028	0.031	0.0230
mLF [28]	0.016	0.026	0.039	0.056	0.0343
Alg [25]	0.015	0.020	0.026	0.040	0.0251
mAlg (this study)	0.020	0.026	0.023	0.024	0.0230

dataset, and find an answer to the question: ‘Which model does give the closest fit to the experimentally measured test data at the lowest expense of computational time, which is directly related to the complexity of the model?’

In total, eight parametric models are considered in this study, three of which are algebraic in nature, and the remaining five models are coupled differential equation systems. In order to estimate the optimal model parameters for Kwok [24], Alg [25] and modified Alg models the Matlab Curve Fitting Toolbox was employed, while the Matlab/Simulink-Parameter Estimation Toolbox (PET) was run for the other models

under consideration. Both toolboxes use a nonlinear least-squares method in order to match model predictions and the experimental data.

In order to make a comparative evaluation among the various models, some error criteria are needed since graphical representations would not be good enough to assess the performance evaluation of each individual model. Spencer *et al* [3] proposed the following error expressions ( $E_t, E_x, E_{\dot{x}}$ ), which are a function of time, displacement and velocity over two complete cycles, respectively:

$$E_t = \sqrt{\frac{\int_0^T (F_{\text{test}} - F_{\text{model}})^2 dt}{\int_0^T (F_{\text{test}} - \mu_F)^2 dt}} \quad (18)$$

$$E_x = \sqrt{\frac{\int_0^T (F_{\text{test}} - F_{\text{model}})^2 \left| \frac{dx}{dt} \right| dt}{\int_0^T (F_{\text{test}} - \mu_F)^2 \left| \frac{dx}{dt} \right| dt}} \quad (19)$$

$$E_{\dot{x}} = \sqrt{\frac{\int_0^T (F_{\text{test}} - F_{\text{model}})^2 \left| \frac{d\dot{x}}{dt} \right| dt}{\int_0^T (F_{\text{test}} - \mu_F)^2 \left| \frac{d\dot{x}}{dt} \right| dt}} \quad (20)$$

where  $F_{\text{test}}$  and  $F_{\text{model}}$  are the experimentally measured and predicted damping forces, respectively.  $\mu_F$  is the average test force during a test period of  $T$ . These normalized errors of four different maximum piston velocities (0.05, 0.10, 0.15 and 0.20 m s<sup>-1</sup>) for eight parametric models are given in table 2. The average values of errors are also provided in the same table to gain an insight about the overall performance of each model. It is clear from table 2 that the algebraic models Kwok [24], Alg [25] and mAlg (present study) exhibited generally better performance than those parametric models which are in differential form. In terms of  $E_t$ , the Kwok [24] model produced the lowest error, which is 0.0221, while the mAlg model (equation (16)) gives an average error of  $E_t = 0.0257$ . It is also evident that the evolution of the BW model from its classical form to its current-dependent modified form led the error norms to decrease remarkably. For example,

the general BW model [3] gives an average  $E_t = 0.0503$ , while its rather improved version gives  $E_t = 0.0241$ , which is nearly half the general BW model. Despite this striking improvement, the algebraic models are still better than those complicated models as show in table 2.

Similar trends were also observed for both  $E_x$  and  $E_{\dot{x}}$ , which represent the resulting normalized error norms associated with displacement and piston velocity, respectively. But this time, the mAlg model proposed in this paper (equation (16)) is seen to be superior to the others, since it effectively predicts the dynamic behavior of the test damper with lowest error norms, e.g.  $E_x = 0.0038$  and  $E_{\dot{x}} = 0.023$  on average.

Table 2 also reveals that the much more complicated differential models, e.g. BW, mBW and vmBW models [3], do not offer any advantage over the existing relatively simple algebraic models at the expense of their complexities, at least for the present damper test data. Therefore simple algebraic parametric models can be safely used to construct control algorithms of such devices at a low expense of computational time. In addition simple algebraic models do not require much expertise in their mathematical manipulations.

In addition to the normalized error norms ( $E_t, E_x, E_{\dot{x}}$ ) proposed by Spencer *et al* [3], the mean and average deviations were also introduced since they have been commonly used to compare experimental measurements and model predictions in a straightforward manner. The mean and average deviations represent the absolute deviation from the observations and the spread of data about the ideal line (which makes a 45° angle with respect to the  $x$  axis) between measured and predicted data, respectively. The expressions of the mean and average deviations are defined as

$$\text{Mean deviation} = \frac{1}{N} \sum_1^N \left| \frac{F_{\text{test}} - F_{\text{model}}}{F_{\text{test}}} \right| \quad (21)$$

$$\text{Average deviation} = \frac{1}{N} \sum_1^N \frac{F_{\text{test}} - F_{\text{model}}}{F_{\text{test}}} \quad (22)$$

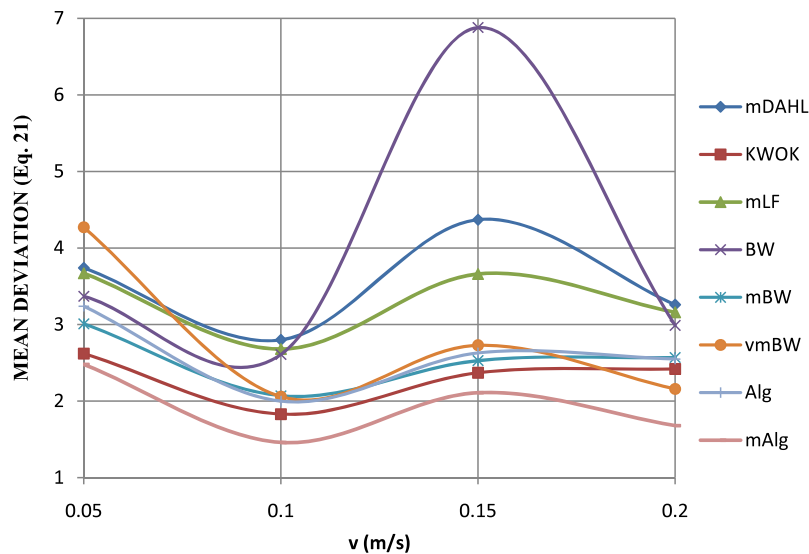


Figure 7. Comparison of percentage mean deviations from test data for the parametric models considered.

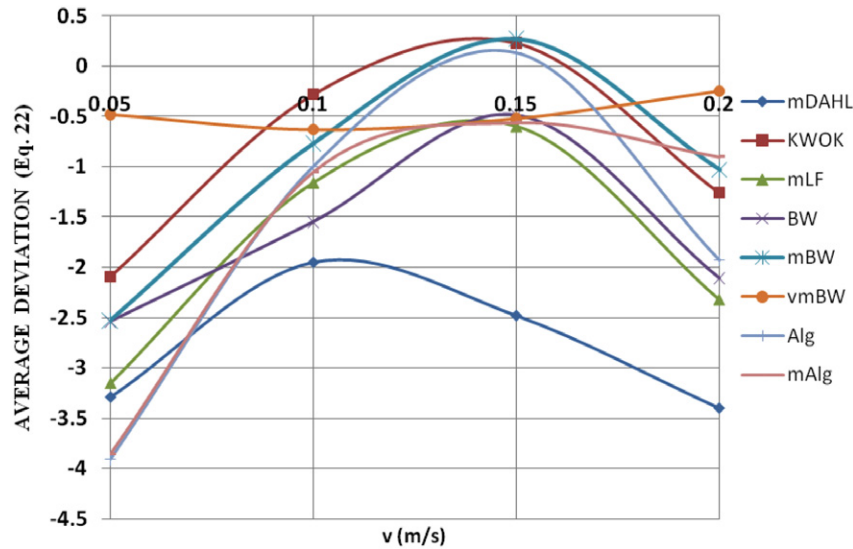


Figure 8. Comparison of percentage average deviations from test data for the parametric models considered.

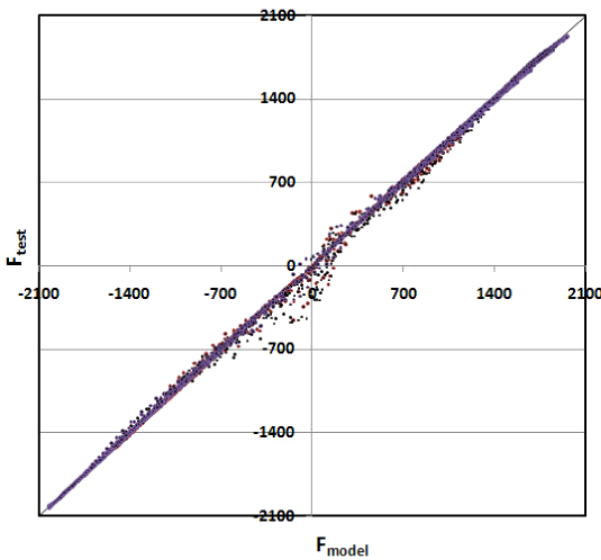


Figure 9. Comparison between measured and predicted data for the proposed mAlg model (equation (16)). The data cover all excitation currents (0–2 A) and velocities (0.05 to 0.20 m s<sup>-1</sup>).

where  $N$  is the number of test data used. The percentage mean and average deviations of eight parametric models are shown in figures 7 and 8, respectively. It is clearly observed from figures 7 and 8 that the mAlg model proposed in this study exhibits the lowest mean deviation among the other seven parametric models. This indicates the superiority of the proposed modification to the original Alg model [25], since it provides nearly a 25% improvement (better prediction on average) over the original version.

As depicted earlier, the average deviation represents the direction and amount of spread of data about the ideal line, which represents the geometric locus of the points at which the measured and predicted values are the same (zero deviation from the measured data). In terms of the average deviation, the mAlg model is generally seen to be closer to the ideal line, which means data are nearly equally distributed about the ideal line, as shown in figure 9. The range of deviation lies generally between  $\pm 5\%$ . This spread could be viewed very reasonable when considering the volume of data and the number of parameters involved.

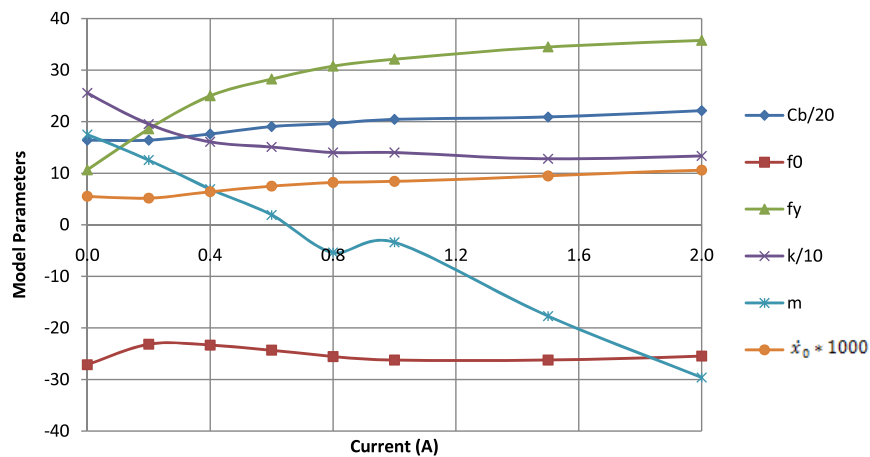


Figure 10. Parameter estimates for the modified algebraic model proposed in this study ( $0.05 \leq \dot{x} \leq 0.2 \text{ m s}^{-1}$ , piston stroke = 25 mm).

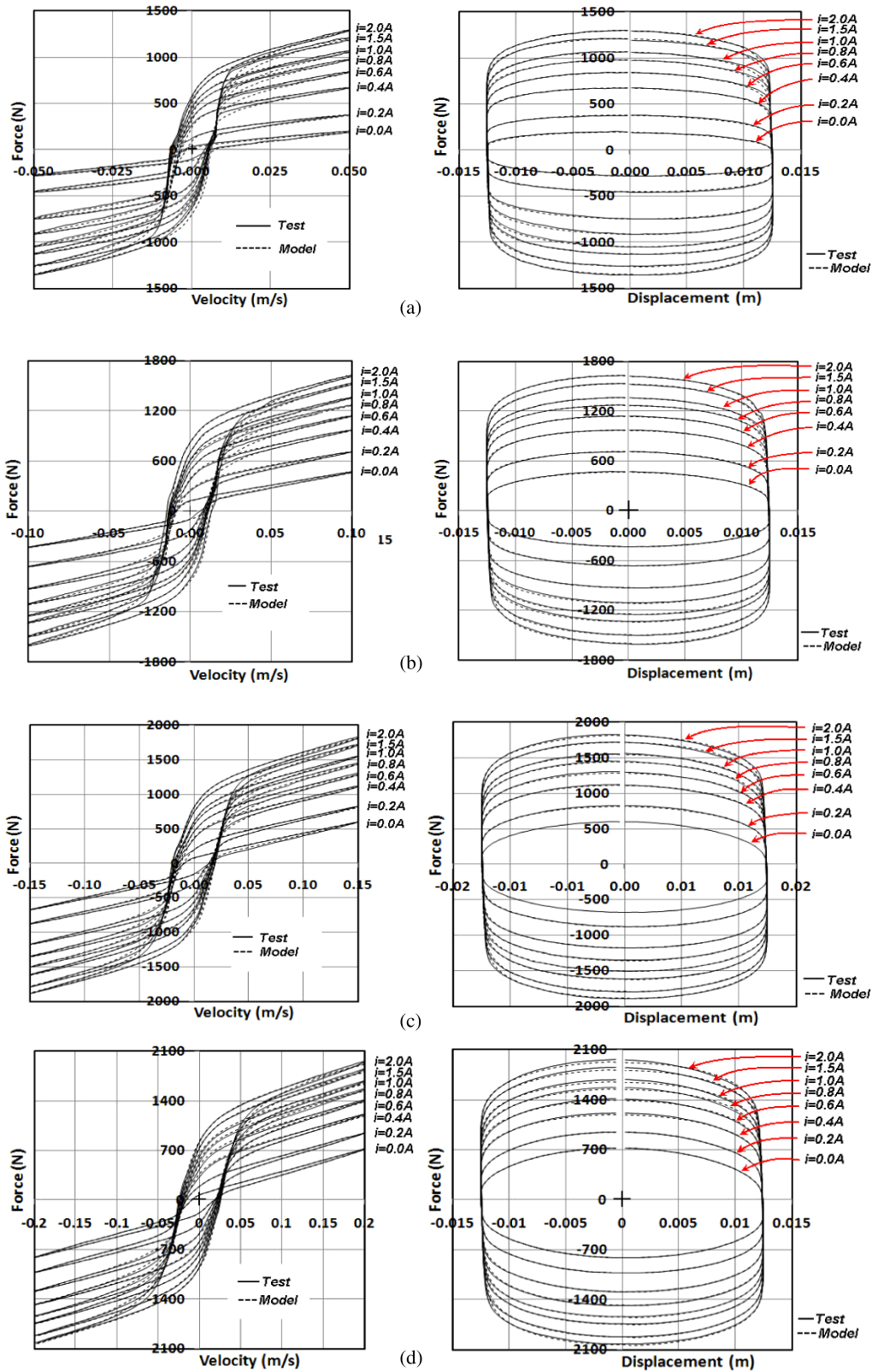


Figure 11. Comparison between the test data and the modified algebraic model (mAlg) for different currents and velocities.

From the above discussions, the Kwok model [24] and the mAlg seemed to have much better prediction performance compared to others, particularly to the differential models. It was also determined that the proposed modified model gives

slightly better predictions than the Kwok model. The variation of model parameters with excitation current for a damper velocity amplitude of  $0.05 \leq \dot{x}_p \leq 0.2 \text{ m s}^{-1}$  and a fixed stroke of 25 mm is shown in figure 10. In order to enhance

the visibility of the variations in the figure, we multiplied  $c_b$  by 1/20,  $k$  by 1/10 and  $\dot{x}_p$  by 1000. It is clearly seen from figure 10 that all parameters, except  $m$ , vary almost linearly with excitation current, particularly at higher currents.

The simulation results generated using the modified algebraic model proposed in this study and their comparisons with the experimental data for a range of maximum piston velocities and excitation currents are illustrated in figures 11(a)–(d). With the modification of Guo's model [25], a remarkable improvement by 25% over the original model has been provided. As can be seen from figures 11(a)–(d), the simulated results are in excellent agreement with the measured data. Therefore it can be concluded the proposed modified algebraic can accurately predict the hysteretic behavior of the damper at all times. It should be noted that the presented results have been obtained for a fixed stroke of 25 mm. However, similar agreements were also observed up to the maximum stroke of the MR damper tested.

## 5. Conclusions

As a semi-active control device, the MR fluid dampers have received significant attention in the last decade due to the rapid variation in the damping properties in a reliable fail-safe manner and low power consumption. The effective control of an MR damper mainly depends on understanding its nonlinear hysteretic behavior under an applied magnetic field. Therefore, the accurate control algorithms that take maximum advantage of the unique features of MR dampers need to be developed using mathematical models that must adequately characterize the intrinsic nonlinear behavior of these devices.

There are several existing parametric models available in the literature proposed to capture nonlinear hysteretic behavior of MR dampers, some of which are in differential form and others are algebraic in nature. Since the ordinary differential-type parametric models, involving generally larger number of parameters, are rather complicated to solve, and the estimating their parameters requires massive computational time due to the frequently occurred divergence problem, the simpler algebraic models became attractive with their (better) accuracies competing against differential models.

In this paper, an MR damper has been designed, fabricated and tested. Then, a comparative evaluation of some existing parametric models using obtained test data has been carried out. A total of eight parametric models, three of which are algebraic and five of which are in ordinary differential equation form, were comparatively examined taking the normalized error norms depicted in the literature, and well-known average and mean deviation relations as a basis. Both error criteria revealed that the simple algebraic parametric models could capture more accurately the nonlinear hysteretic behavior of the MR damper tested, and the differential parametric models commit no appreciable advantage over the algebraic models at the expense of their complexity and massive time-consuming for finding their larger number of model parameters.

Moreover, an existing algebraic model [25] has been modified by adding a simple inertial term so that it can capture the damper behaviour at low piston velocities as

well. By doing this, a remarkable improvement by 25% over the original model has been provided. It was showed that excellent agreement was present between the simulated results generated by employing the modified algebraic model and the experimental results. Therefore we conclude that the modified algebraic parametric model (equation (16)) can be safely used for developing control algorithms of automotive suspension systems and adaptive structures requiring semi-active vibration control, owing to its reliability and capability of predicting the hysteresis force accurately at any excitation conditions. Nevertheless, it should be noted that, ultimately, the differences in the various models considered in this paper are relatively small, and may not be significant from a practical point of view.

## Acknowledgment

This research is fully supported by The Scientific and Technological Research Council of Turkey (TÜBİTAK) under grant nos 108M635 and 104M157.

## References

- [1] Kim Y, Langari R and Hurlebaus S 2009 Semiactive nonlinear control of a building with magnetorheological damper system *Mech. Syst. Signal Process.* **23** 300–15
- [2] Claudio C and Donha D C 2008 Discrete-time dynamic model of a magneto-rheological damper for semi-active control design *ABCMSymp. Ser. Mechatron.* **3** 27–36
- [3] Spencer B F, Dyke S J, Sain M K and Carlson J D 1997 Phenomenological model of a magnetorheological damper *ASCE J. Eng. Mech.* **123** 230–8
- [4] Boada M J L, Calvo J A, Boada B L and Diaz V 2008 Modeling of a Magnetorheological damper by recursive lazy learning *Int. J. Non-Linear Mech.* at press (doi:10.1016/j.ijnonlinmec.2008.11.019)
- [5] Ehrgott R C and Masri S F 1992 Modeling the oscillatory dynamic behavior of electrorheological materials in shear *Smart Mater. Struct.* **1** 275–85
- [6] Gavin H P, Hanson R D and Filisko F E 1996 Electrorheological dampers, part ii: testing and modeling *J. Appl. Mech.* **63** 676–82
- [7] Chang C C and Roschke P 1998 Neural network modeling of a magnetorheological damper *J. Intell. Mater. Syst. Struct.* **9** 755–64
- [8] Chang C C and Zhou L 2002 Neural network emulation of inverse dynamics for a magnetorheological damper *J. Struct. Eng.* **128** 231–9
- [9] Wang D H and Liao W H 2004 Modeling and control of magnetorheological fluid dampers using neural networks *Smart Mater. Struct.* **14** 111–26
- [10] Du H, Lam J and Zhang N 2006 Modeling of a magneto-rheological damper by evolving radial basis function networks *Eng. Appl. Artif. Intell.* **19** 869–81
- [11] Schurter K C and Roschke P N 2000 Fuzzy modeling of a magnetorheological damper using Anfis *Proc. IEEE Int. Conf. on Fuzzy Systems* pp 122–7
- [12] Wilson C M D and Abdullah M 2005 Structural vibration reduction using fuzzy control of magnetorheological dampers *ASCE Structures Congr. (New York)*
- [13] Stanway R, Sproston J L and Stevens N G 1987 Non-linear modeling of an electrorheological vibration damper *J. Electrosta.* **20**
- [14] Gamota D R and Filisko F E 1991 Dynamic mechanical studies of electrorheological materials: moderate frequencies *J. Rheol.* **35** 399–425

- [15] Wereley N M, Pang L and Kamath G M 1998 Idealized hysteresis modeling of electrorheological and magnetorheological dampers *J. Intell. Mater. Syst. Struct.* **9** 642–9
- [16] Kamath G M and Wereley N M 1997 A nonlinear viscoelastic-plastic model for electrorheological fluids *Smart Mater. Struct.* **6** 351–9
- [17] Li W H, Yao G Z, Chen G, Yeo S H and Yap F F 2000 Testing and modeling of a linear MR damper under sinusoidal loading *Smart Mater. Struct.* **9** 95
- [18] Choi S B, Lee S K and Park Y P 2001 A hysteresis model for the field-dependent damping force of a magnetorheological damper *J. Sound Vib.* **245** 375–83
- [19] Gavin H, Hoagg J and Dobossy M 2001 Optimal design of MR dampers *Japan Workshop on Smart Structures For Improved Seismic Performance in Urban Regions (Seattle)* pp 225–36
- [20] Wen Y K 1976 Method of random vibration of hysteretic systems *ASCE J. Eng. Mech. Div.* **102** 249–63
- [21] Domingez A, Sedaghati R and Stiharu I 2006 A new dynamic hysteresis model for magnetorheological dampers *Smart Mater. Struct.* **15** 1179–89
- [22] Zhou Q, Nielsena S R K and Qu W L 2006 Semi-active control of three-dimensional vibrations of an inclined sag cable with magnetorheological dampers *J. Sound Vib.* **296** 1–22
- [23] Dahl P R 1976 Solid friction damping of mechanical vibrations *AIAA J.* **14** 1675–82
- [24] Kwok N M, Ha Q P, Nguyen T H, Li J and Samali B 2006 A novel hysteretic model for magnetorheological fluid dampers and parameter identification using particle swarm optimization *Sensors Actuators A* **132** 441–51
- [25] Guo D and Hu H 2005 Nonlinear-stiffness of a magnetorheological fluid damper *Nonlinear Dyn.* **40** 241–9
- [26] Gavin H P 2001 Multi-duct ER dampers *J. Intell. Mater. Syst. Struct.* **12** 353
- [27] Alvarez L and Jimenez R 2002 Real-time identification of magneto-rheological dampers *Proc. 15th Triennial IFAC World Congr.* Paper 2252
- [28] Jimenez R and Alvarez-Icaza L 2005 LuGre friction model for a magnetorheological damper *Struct. Control Health Monit.* **12** 91–116